Published in final edited form as:
J Biol Chem. 2008 May 16; 283(20): 14132–14143. doi:10.1074/jbc.M708034200.

p21-activated Kinase-aberrant Activation and Translocation in Alzheimer Disease Pathogenesis*

Qiu-Lan Ma[‡,§], **Fusheng Yang**[‡,§], **Frédéric Calon**[¶,•], **Oliver J. Ubeda**[‡,§], **James E. Hansen**[‡,§], **Richard H. Weisbart**[‡,§], **Walter Beech**[‡,§], **Sally A. Frautschy**[‡,§,**], and **Greg M. Cole**[‡,§,**1]

‡*Department of Medicine, UCLA, Los Angeles, California*

***Department of Neurology, UCLA, Los Angeles, California*

§*Geriatric Research and Clinical Center, Greater Los Angeles Veterans Affairs Healthcare System, Veterans Affairs Medical Center, North Hills, California 91343*

¶*Molecular Endocrinology and Oncology Research Center, Laval University Medical Center, Québec City, Québec G1V 4G2, Canada*

•*Faculty of Pharmacy, Laval University, Québec City, Québec G1K 7P4, Canada*

Abstract

Defects in dendritic spines and synapses contribute to cognitive deficits in mental retardation syndromes and, potentially, Alzheimer disease. p21-activated kinases (PAKs) regulate actin filaments and morphogenesis of dendritic spines regulated by the Rho family GTPases Rac and Cdc42. We previously reported that active PAK was markedly reduced in Alzheimer disease cytosol, accompanied by downstream loss of the spine actin-regulatory protein Drebrin. •-Amyloid (A•) oligomer was implicated in PAK defects. Here we demonstrate that PAK is aberrantly activated and translocated from cytosol to membrane in Alzheimer disease brain and in 22-month-old Tg2576 transgenic mice with Alzheimer disease. This active PAK co-immunoprecipitated with the small GTPase Rac and both translocated to granules. A• $_{42}$ oligomer treatment of cultured hippocampal neurons induced similar effects, accompanied by reduction of dendrites thatwere protected by kinase-active but not kinase-dead PAK. A• $_{42}$ oligomer treatment also significantly reduced N-methyl-D-aspartic acid receptor subunit NR2B phosphotyrosine labeling. The Src family tyrosine kinase inhibitor PP2 significantly blocked the PAK/Rac translocation but not the loss of p-NR2B in A• $_{42}$ oligomer-treated neurons. Src family kinases are known to phosphorylate the Rac activator Tiam1, which has recently been shown to be A•-responsive. In addition, anti-oligomer curcumin comparatively suppressed PAK translocation in aged Tg2576 transgenic mice with Alzheimer amyloid pathology and in A• $_{42}$ oligomer-treated cultured hippocampal neurons. Our results implicate aberrant PAK in A• oligomer-induced signaling and synaptic deficits in Alzheimer disease.

*This work was supported, in whole or in part, by National Institutes of Health Grants AG16570 (to G. M. C.), AG13471 (to G. M. C.), U0128583 (to S. A. F.), and AG021975 (to S. A. F.). This work was also supported by National Center on Complementary and Alternative Medicine Grant AT003008 (to G. M. C.) and Alzheimer Association Grant NIRG-07–59659 (to Q.-L. M.).

1To whom correspondence should be addressed: Greater Los Angeles Veterans Affairs Healthcare System Alzheimer Research-151, Bldg. 7, Rm. A102, 16111 Plummer St., North Hills, CA 91343. Fax: 818-895-5835; E-mail: gmcole@ucla.edu.

Cognitive deficits in Alzheimer disease (AD)[2] correlate with progressive synaptic dysfunction and loss that may be initiated by soluble •-amyloid peptide 1–42 (A• $_{42}$) and driven further by the accumulating neuropathological hallmarks, including intraneuronal neurofibrillary tangles, extracellular amyloid plaques, and neuron loss. Soluble A• or A• oligomers correlate highly with synapse loss (1,2) and the degree of dementia (3). They also potently inhibit long term potentiation (LTP) in vivo (4). A•-induced synaptic dysfunction likely contributes to cognitive deficits in several different AD transgenic mouse models (5–7).

Both dystrophic neurites and dendritic spine loss are observed in AD and many mental retardation syndromes (8–10). Dendritic spines, major sites of synaptic contacts, are structurally reliant on the actin cytoskeleton. p21-activated kinases (PAK) (11) are a family of serine/threonine protein kinases involved in regulating the actin-severing protein cofilin, the actin cytoskeleton, and dendritic function as downstream effectors of Rac1/Cdc42 (12). Thus, the small GTPases (Rho, Rac, and Cdc42) play critical roles in regulating dendrite initiation, growth, branching, spinogenesis, and spine maintenance (13–15). Mutations in PAK3 are associated with X-linked non-syndromic forms of mental retardation, in which the only distinctive clinical feature is severe cognitive deficits (16). Inhibition of PAK is sufficient to cause cognition impairment in dominant-negative PAK transgenics (17) and adult mice (18).

We have previously observed that PAKs (PAK1 and PAK3) and PAK activity are markedly reduced in cytosol from AD, accompanied by prominent cofilin pathology and downstream loss of the spine actin-regulatory protein Drebrin; A• oligomer was implicated in these alterations (18), but the cause of the loss of cytosolic PAK and its impact on spine generation were not understood.

In this study, we report that AD cytosolic PAK loss occurs because of aberrant PAK activation and translocation to membrano-cytoskeletal fractions where it co-localizes with its activating GTPase Rac1. These phenomena were also observed in Tg2576 transgenic AD model mice and in A• $_{42}$ oligomer-treated primary neurons where PAK changes were accompanied by rapid loss of F-actin and the postsynaptic marker PSD-95. These changes were treatable with curcumin, a natural anti-A• compound extracted from turmeric spice.

EXPERIMENTAL PROCEDURES

Chemicals and Reagents

All chemicals, including the anti-NR2B subunit Tyr(P)-1472 antibody, were purchased from Sigma, unless otherwise stated. We used anti-PAK1 polyclonal antibody (pAb) from Zymed Laboratories Inc., anti-PAK3 pAb from StressGen Biotechnologies (Victoria, British Columbia, Canada), and anti-•-actin monoclonal antibody from Chemicon International (Temecula, CA). Anti-PAK1,2,3 pAb, anti-phospho-PAK Thr-423 pAb, which detects PAK1, PAK2, and PAK3 only when phosphorylated at Thr-423, -402, and -421, respectively ("pPAK"), does not cross-react with phosphorylated PAK4, PAK5, or PAK6 from Cell Signaling Technology (Danvers, MA). Anti-phospho-Ser-71-Rac/Cdc42 pAb was also from Cell Signaling Technology. Anti-A•-pAb (DAE) was developed and characterized in our laboratory. Anti-A• monoclonal antibody 6E10 was obtained from Signet Laboratories, Inc. (Dedham, MA). A•-(1–42) peptide was from American Peptide Co. (Sunnyvale, CA). PP2 was obtained from Calbiochem. The red fluorescent F-actin probe, Texas red-X-phalloidin was from Molecular Probes (Eugene, OR).

[2]The abbreviations used are: AD, Alzheimer disease; A• $_{42}$, •-amyloid peptide-(1–42); ICC, immunocytochemistry; LTP, long term potentiation; PAK, p21-activated kinases; pAb, polyclonal antibody; pPAK, phosphorylated-PAK; WT, wild type; DTT, dithiothreitol; Tricine, N-[2-hydroxy-1,1-bis(hydroxymethyl)ethyl]glycine; TBS, Tris-buffered saline; GFP, green fluorescent protein; NMDA, N-methyl-D-aspartic acid; PSD, postsynaptic density; DIV, days in vitro; APP, amyloid precursor protein.

Human Tissue

Human postmortem tissue was obtained from the University of Southern California (Dr. Carole Miller) and UCLA (Dr. Harry Vinters) AD Research Center Pathology Cores. Five AD patients and five controls were used in this experiment. The age of death, gender, and post-mortem interval were comparable in both groups.

Animals

22-Month-old APPswe Tg2576 Tg• (n • 5) and Tg• (n• 7) mice were used in this study. Both groups were fed from 17 months with safflower oil-based diet depleted of n-3 polyunsaturated fatty acids (TD 00522, Harlan Teklad, Madison, WI) as described previously (19). Surgical and animal procedures were approved by the local Institutional Animal Care Use Committee and carried out with strict adherence to the current guidelines set out in the NIH Guide for the Care and Use of Laboratory Animals at the Association for Assessment and Accreditation of Laboratory Animal Care-accredited Greater Los Angeles Veterans Affairs Healthcare System.

Tissue Preparation

Tissue samples were sequentially processed by sonication in Tris-buffered saline (TBS) and ultracentrifugation (100,000 • g for 20 min) to obtain supernatants (TBS, soluble-cytosol fraction). Pellets were then sonicated in immunoprecipitation lysis buffer containing 1% Triton X-100, 0.5% sodium deoxycholate, and 0.5% SDS and re-centrifuged to obtain lysis extract supernatants (membrano-cytoskeletal extract). Alternatively, TBS pellets were extracted in 2% SDS buffer to extract membrane and additional Triton-insoluble components, mostly cytoskeletal-associated proteins (SDS fraction). All buffers contained previously described protease inhibitor and phosphatase inhibitor mixtures (19).

Preparation of Oligomers

A•-(1–42) peptide (A• $_{42}$)was dissolved in 1,1,1,3,3,3-hexafluoro-2-propanol in the vial and incubated at room temperature until dissolved completely. The 1,1,1,3,3,3-hexafluoro-2-propanol was removed by gentle streaming of N_2. A• $_{42}$ was then dissolved with 10 mM HEPES (pH 7.4) to a final concentration of 110 • M. This solution was incubated at 37 °C with a micro stir bar at 500 rpm for 12 h and centrifuged at 14,000• g for 5 min to remove fibrillar and other large A• aggregates. The presence of A• oligomers was confirmed by 6E10 anti-A• antibody following its separation on 10–20% Tris-Tricine gradient gels (20). Protein concentration was determined using the Bio-Rad DC protein assay. For cell culture experiments, the oligomer-rich supernatant preparation was diluted to 100 or 250 nM in Neurobasal media without glutamate and B27.

Primary Neuronal Culture and Treatment

Neuronal cultures were prepared from embryonic day 18 Sprague-Dawley rat fetuses as described previously (18). Before treatment with A• oligomer preparations, cells were rinsed once with Neurobasal media without glutamate and B27 for primary neurons. Cells were exposed to 100 or 250 nM of A• $_{42}$ oligomers for 30 min to 48 h at 37 °C.

Plasmids and Transient Transfection

Green fluorescent protein-tagged pcDNA3-EGFP-vector (Vector Laboratories), pcDNA3-EGFP-Pak1-WT (WT-PAK), and pcDNA3-EGFPPAK1-K299A (KD-PAK) constructs were kind gifts of Dr. G. M. Bokoch (The Scripps Research Institute, La Jolla, CA). Primary hippocampal neurons (19 days) were plated onto coverslips in 15.6-mm dishes and were transfected for 24 h using Lipofectamine™ 2000 (Invitrogen) according to the manufacturer's protocol. 1.2 • g of expression plasmid and 2 • l of Lipofectamine 2000 were used for

transfection in 500 • l of medium per well. After transient transfection for 24 h, 100–250 n_M of A• $_{42}$ oligomers were directly added to the cells and incubated for 2.5 h at 37 °C. The cells were then fixed with 4% formaldehyde for 10 min at room temperature, washed with TBS, and stained with Texas-red-X-phalloidin (F-actin) and pRac/Cdc42 antibody.

Cell Lysate Preparation

Primary neurons were placed on ice, washed once with cold PBS, scraped with 1 ml of PBS, and transferred to microcentrifuge tubes. After centrifugation at 1,000 rpm for 5 min, cells were washed twice with cold PBS and dissolved in TBS buffer with a mixture of protease and phosphatase inhibitors. After brief sonication, the lysates were kept at 4 °C for 30 min and centrifuged at 14,000 rpm for 10 min, and the supernatants were collected for TBS fraction (cytosol fraction). The pellet was dissolved in lysis buffer with a mixture of protease and phosphatase inhibitors, sonicated, and centrifuged to extract lysis fractions (membrane fractions).

Western Immunoblotting

For Western immunoblotting, protein concentration was determined using the Bio-Rad DC protein assay. Equal amounts of protein per sample were added to Laemmli loading buffer and boiled for 3 min. Except for A• oligomer detection, 30 • g of protein per well was electrophoresed on 10% Tris-glycine gels and transferred to Immobilon-P polyvinylidene difluoride membranes (Millipore, Bedford, MA). For A• species separation, the protein samples were electrophoresed on 10–20% Tris-Tricine gradient gels (20).

Statistical Analysis

Statistical analyses were performed with StatView 5.0 software. Differences among means were assessed by analysis of variance followed by Tukey-Kramer post hoc tests. Square root transformation to establish homogeneity of variance was used as needed for data analysis.

RESULTS

PAK-aberrant Translocation in Alzheimer Disease

Our previous study found markedly reduced diffuse (cytosolic) pPAK423 and pPAK141 in AD, but also intense and abnormally focal pPAKs in granular intraneuronal structures (18). In this study, we hypothesized that this abnormal granular pPAK could result from oligomer-induced aberrant activation and translocation. To test this hypothesis, we first examined the PAK1 and PAK3 levels from pellet membrano-cytoskeletal fractions (Lysis and SDS buffer extracted fractions) in AD temporal cortex (Fig. 1A). Our results showed that both PAK1 and -3 levels were significantly higher in pellet fractions from AD patients than that of controls (*, p • 0.05; **, p • 0.01, respectively, Fig. 1, B and C). Because phosphorylation of Thr-423 is critical for PAK1 activation (21) and analogously Thr-402 (PAK2) and Thr-421 (PAK3), an anti-phospho-PAK (pPAK) antibody recognizing these forms was used to evaluate levels of active PAK1–3, which showed significant increases in the pellet fraction from AD when compared with controls (*, p • 0.05, Fig. 1D) with no change in •-actin. In samples from the same patients, PAK1, PAK3, and active PAKs (pPAK) were decreased in cytosolic TBS fractions (PAK1,*, p • 0.05; PAK3, pPAK, **, p • 0.01, Fig. 1, E–H). The ratio of membrane to cytosol active pPAK from AD patients was significantly elevated (**, p• 0.01, Fig. 1I), supporting ICC results suggesting aberrant neuronal pPAK translocation in AD (Fig. 1M).

To determine whether pPAK translocation in AD was associated with a known activator, we next investigated Rac/Cdc42, small GTPases known to regulate PAK activity. Pooled (n • 5) membrane pellet fractions extracted with immunoprecipitation lysis buffer from AD or normal

human hippocampi were immunoprecipitated with an anti-PAK1–3 antibody, followed by Western blotting for pPAK, pRac1, and PAK1–3. Levels of both 65–70-kDa pPAKs and pRac1 were increased in immunoprecipitates from membrane pellet fractions of AD patients as compared with controls, suggesting active PAK was co-translocated interacting with Rac1 in AD brain. Consistent with these results, a strong higher molecular mass pPAK immunoreactive band between 160 and 250 kDa from the same blot was also clearly increased in AD pellet samples (Fig. 1J), suggesting translocation of a PAK complex. To further analyze whether the higher molecular weight pPAK immunoreactive band is a PAK complex, DTT was added to reduce the same samples before running gels. The higher molecular weight pPAK band present on our standard weakly reducing gels (with 2-mercaptoethanol, but without DTT and boiling; Fig. 1K, left lane) was completely broken down to the 65–70-kDa PAK monomers under strong reducing conditions (with DTT and boiling, Fig. 1K, right lane). To confirm that pPAK-reactive higher molecular weight bands contained PAK rather than cross-reactive bands, PAK3-specific antibodies were used to show a high molecular weight PAK3 immunoreactive band observed on standard Western blots that was also elevated in membrane fractions but decreased in cytosol fractions from pooled individual AD when compared with normal samples (Fig. 1L). Immunofluorescence analysis with anti-phospho-Rac1/Cdc42Ser-71 (pRac/Cdc42) and pPAK antibodies showed that abnormal granular pPAK largely co-localized with pRac/Cdc42 in the hippocampus of AD patients. In contrast, normal control hippocampus exhibited only diffuse neuronal pPAK and p-Rac (Fig. 1M). Co-localization of discrete structures was not detected.

PAK Translocation in APPsw Tg2576 Mice

Cytosolic PAK deficits and aberrant PAK translocation in AD could be secondary to neuron loss and tau pathology or antemortem and postmortem conditions. Therefore, we used APPsw Tg2576 AD model mice that lack significant neuron loss and tau pathology and where post-mortem conditions can be controlled. In our previous study with diaminobenzidine immunohistochemical staining of 22-month-old Tg2576 mice, we observed that pPAK labeling of neurons was uneven with a loss of diffuse neuronal staining but with patches of intense staining. We found plaque-associated labeling of dystrophic neurites and clusters of neuron staining, frequently showing granular or flame-shaped inclusions (18). Here we used different groups of 22-month-old outbred aged transgene-positive or control negative mice placed for the last 5 months on a safflower oil-based omega-3 fatty acid-depleting diet that we had previously found to enhance A• accumulation and postsynaptic pathology (19). We found that pPAK immunofluorescent staining revealed similar granular structures and a loss of diffuse pPAK in the aged Tg2576 transgene-positive mice but remained diffuse and apparently cytosolic in wild type (transgene-negative)mice with the same age and genetic background (Fig. 2A). To further confirm pPAK translocation in Tg2576 mice, we examined the levels of pPAK from membrane and cytosol fractions in these aged 22-month-old Tg2576 mice. pPAK levels in membrane and cytosol fractions were significantly lower in Tg2576 mice than controls (*, p • 0.05; ***, p • 0.001 respectively, Fig. 2, B and C). The pPAK ratio of membrane to cytosol was significantly increased in Tg2576-positive mice when compared with controls (**, p • 0.01, Fig. 2D), similar to the observations in AD patients (Fig. 1). Therefore, aberrant PAK activation and translocation occur in both AD and aged tangle-free Tg2576 transgenic mice, suggesting that A• aggregates could account for these abnormalities. To prove that A• rather than APP or another APP metabolite was responsible for the PAK effects, we explored direct application of synthetic $A•_{42}$ in vitro.

Characterization of A• Oligomers

Analysis of our soluble A• “oligomer” preparations showed about 58% of $A•_{42}$ converted to 12- and 24-mer, 34% of $A•_{42}$ converted to 3- or 4-mer, whereas only 8% of $A•_{42}$ remained in monomer status, which was characterized by silver stain and 4G8 anti-A• antibody as reported previously (20) (also see Fig. 3F). Arguing for active toxic oligomer species, both

trimer and hexamer (22) or A• *56 (23), the main component in our oligomer preparations, have been proposed as key forms of A• responsible for cognitive deficits in vivo. Moreover, these A• $_{42}$ preparations significantly induced phospho-PAK141 and Drebrin loss at 100–500 n_M doses in cultured hippocampal neurons and activated the tau kinase, GSK3•, in human SH-SY5Y cell lines, and these effects were prevented by pretreatment with oligomer-specific A11 antibody that does not bind to fibrils or monomer (18,20,24).

Oligomer Treatment and PAK Aberrant Activation and Translocation in Primary Neurons

Hippocampal neurons cultured 7 days in vitro (7 DIV) were treated with 100 n_M soluble A• $_{42}$ oligomer preparations, and pPAK was examined. After 30–120 min of treatment, the active PAK assessed by immunostaining of phosphorylation at the Thr-423 site was elevated, and this pPAK was apparently translocated from diffuse perikaryal to membrane and neurites (Fig. 3A). Punctate anti-A• antibody staining decorated neuronal cell bodies and processes, similar to the synaptic pattern obtained with soluble A• oligomers extracted from human AD brain (25). When 7 DIV hippocampal neurons were treated with 250 n_M A• oligomers for 30 min • 5 h and Western-blotted with anti-pPAK Thr-423 antibody, pPAK levels were significantly increased in membrane and cytosol fractions when compared with controls (*, p • 0.05, and ***, p • 0.001, Fig. 3, B and C, 30 min), and the pPAK ratio of membrane to cytosol had a trend increase (p • 0.063, Fig. 3D, 30 min). Similar data were obtained at 2–5 h (not shown). However, an oligomer-induced decrease in cytosolic PAK was evident with longer exposure (9.5–48 h). Fig. 3, E and F, shows the decrease at 9.5 h in membrane and cytosol fractions, whereas Fig. 3G shows the membrane/cytosol ratio is no longer shifted. These observations of reductions in soluble pPAK with more chronic oligomer exposure better resembled those found in AD patients (Fig. 1) and in aged Tg2576 mice (Fig. 2). Together with data showing that passive anti-A• antibody coordinately reduces oligomers and soluble PAK deficits in Tg2576 (18), these data strongly support the hypothesis that PAK signaling defects and co-translocation of a PAK-Rac1-Cdc42 complex in AD brain and Tg2576 are caused by A• oligomers.

A• Oligomer Reduced Dendrites and Dendritic Spines in Primary Neurons

A• oligomer-induced abnormal PAK activation and translocation could disrupt the normal PAK signaling pathways in oligomer-binding excitatory neurons resulting in either too much or too little F-actin assembly and affect morphogenesis of dendrites, dendritic spines and synapses. To test these end points, we examined dendrites and dendritic spines in A• oligomer-treated and control neurons by immunocytochemical staining with Texas red-X-phalloidin, a red fluorescent F-actin stain and anti-PSD-95, a marker for postsynaptic densities (PSDs) in excitatory neurons (Fig. 4). Fig. 4A shows that in hippocampal neurons 19 DIV with robust neuritic outgrowth and mature synapses, A• oligomer- treatment for 7 h resulted in a gross loss in the density of F-actin-labeled dendrites and dendritic spines (***, p • 0.001, Fig. 4, A, C and D). Similar oligomer-induced loss of excitatory PSDs was also revealed by anti-PSD-95 staining (***, p • 0.001, Fig. 4, B,C, and E). A• oligomer-induced spine loss is consistent with alterations found in AD brain and in transgenic mouse AD models (19,26,27) and in vitro models with oligomer treatments (28), further supporting the hypothesis that oligomer-induced deficits may play a significant role in synaptic dysfunction and synapse loss in AD.

Active PAK, but Not Kinase-dead PAK, Protected against A• Oligomer-induced Reduction of Dendrites in Primary Neurons

PAK is a key component in regulating synaptic architecture in postsynaptic protein localization (29), axon guidance (30), and ephrinB1-induced spine formation (31). Because oligomers can both aberrantly activate PAK and cause a loss of cytosolic PAK, we sought to explore whether under- or overexpression of PAK would protect against oligomer-induced dendritic F-actin

changes. To examine this, hippocampal neurons 7 DIV were transfected with wild type PAK1 (WT-PAK), treated with 100 nM A• oligomers, and stained for F-actin. Fig. 5 illustrates strong F-actin labeling in cell bodies and neurites of transfected and nontransfected neurons without oligomers (Fig. 5, A, C, and E) that was significantly reduced after A• oligomer treatment (***, p • 0.001, Fig. 5, B, D and F). In neurons transfected with WT-PAK1, dendritic F-actin staining was better maintained after A• oligomer treatment, with preservation of the normal neuronal architecture compared with adjacent nontransfected cells (***, p • 0.001, Fig. 5, C and D). In contrast, GFP vector-transfected neurons or kinase-dead PAK1 (KD-PAK)-transfected neurons did not show any protective effect from A• $_{42}$ oligomer-induced F-actin loss compared with adjacent neurons (Fig. 5, B and F), implying maintenance of PAK1 activity was sufficient to protect the actin cytoskeleton supporting spines.

Src Family Tyrosine Kinase Inhibitor PP2 Significantly Blocked pPAK Translocation in A• Oligomer-treated Primary Neurons

In addition to PAK, various kinases have been reported as A• mediators. Because the Src family tyrosine kinase Fyn has been implicated in soluble oligomer (amyloid-derived diffusible ligands)-induced LTP defects in vitro (32) and synaptotoxicity and cognitive deficits in APP transgenic mice (33), we investigated whether oligomer-induced Rac/PAK changes in primary hippocampal neurons might be downstream from Fyn. Fig. 6 shows that inhibition of Src/Fyn kinase with PP2 blocked punctate oligomer-induced pPAK up-regulation, notably in granular locations along neurites determined by ICC (Fig. 6A). Western blot analysis of membrane and cytosolic fractions revealed that pPAK translocation from cytosol to membrane induced by A• $_{42}$ oligomers was blocked by the Src/Fyn inhibitor PP2 (Fig. 6, B–D). Similar Western analysis of Rac1 showed translocation from cytosol to the membrane induced by A• $_{42}$ oligomers that was also blocked by PP2 (Fig. 6, E–G).

NMDA receptors have recently been reported to mediate A• oligomer-induced effects on dendritic spine and synaptic marker loss in cultured neurons (2,28). Fyn kinase phosphorylates NMDA receptor subunits NR2A and NR2B in vitro and in vivo, and robust phosphorylation at NR2B Tyr-1472 has been implicated in LTP (34). Oligomer treatment decreased pNR2B (Tyr-1472) levels in both membrane and cytosol fractions but did not alter the membrane/cytosol ratio (Fig. 6, H–J). In contrast to pPAK, Src/Fyn inhibition did not block these oligomer effects, consistent with Fyn activation as independent of or downstream from A• -induced pNR2B loss.

Curcumin Reduced pPAK Translocation in Tg2576 Mice and in A• Oligomer-treated Primary Neurons

PAK activity is involved in actin dynamics in many cell types potentially limiting its utility as a direct drug target. Furthermore, A• oligomers caused pPAK increases in pellet fractions but pPAK decreases in soluble fractions, e.g. translocation, suggesting that the most effective treatment will be to target upstream A• oligomers. Our previous studies found that curcumin is an effective anti-amyloid and anti-A• oligomer agent in vitro (35). Chronic dietary curcumin lowered amyloid burden and A• by ELISA in TBS-soluble and detergent-insoluble fractions from 16-month-old Tg2576 mice (36) and from 22-month-old Tg2576 mice that were fed with safflower oil-based diet from 17 months of age (35). Consistent with this, curcumin (0.5 • M) suppressed punctate anti-A• staining and pPAK translocation induced by A• $_{42}$ oligomers and evaluated by ICC in cultured hippocampal neurons (Fig. 7A). Granular staining was quantified by automated analysis (Image-Pro Plus software) of particulate clusters, and heterogeneity was significantly increased by A• and blocked by curcumin (Fig. 7C). Western analysis of whole cell lysates with oligomer treatment at five time points taken from 9.5 to 48 h showed a consistent oligomer-induced decrease in total cytosolic active PAK (pPAK) that was blocked by pretreatment with curcumin (Fig. 7D). In vivo, curcumin also suppressed persistent pPAK

translocation to granules in CA1 neurons evaluated in aged Tg2576 mice (Fig. 7, B and E). The mice were fed from 17 months of age with safflower oil-based diet with or without 500 ppm curcumin (35). Anti-pPAK immunofluorescence staining was diffuse in control hippocampal CA1, but in CA1 of Tg2576 Tg• mice, pPAK showed translocation to granular structures resembling those found in AD CA1 (see Fig. 1). As with the in vitro experiment, quantitative analysis of both clusters and heterogeneity showed large increases in Tg• mice that were significantly reduced by dietary curcumin.

DISCUSSION

In this study, we explored the mechanism of PAK signaling deficits using AD brain tissue and APPsw Tg2576 transgenic mice. We found PAK signaling deficits resulting from A• $_{42}$ oligomer-induced aberrant PAK activation and translocation, followed by cytosolic pPAK deficits and loss of the excitatory postsynaptic protein PSD-95 and F-actin-labeled dendritic spines. Supporting aberrant PAK activation in AD brain, we found that Rac, the upstream small GTPase activator of PAK, co-immunoprecipitated with pPAK. Immunocytochemistry of both AD brain and AD models confirmed aberrant pPAK co-localization with the upstream activator Rac. Observations in Tg2576 mice and A• $_{42}$-oligomer treated neurons indicated that A• $_{42}$-oligomer may be sufficient to cause PAK signaling defects in AD. Moreover, unlike normal synaptogenic PAK activity, which promotes F-actin assembly and new PSD-95 positive synapses, this oligomer-induced aberrant Rac/PAK activation on PSD-95 positive oligomer-binding excitatory neurons results in ectopic PAK translocation accompanied by rapid alterations in dendritic morphology and the loss of F-actin and dendritic spines.

The Rho family of small GTPases, including Rho, Rac, and Cdc42, has distinct functions in regulating dendritic spines and branches that are vital for their maintenance and reorganization in maturing neurons (37). Mutations that alter Rac and Rho signaling resulted in abnormal neuronal connectivity and cognitive deficits in humans (38). PAK activity and its subcellular distribution are tightly regulated by rapid and transient localized Rac and Cdc42 activation. Here we found that in AD brain an abnormal granular distribution of pPAK was co-localized with pRac/Cdc42 in the hippocampus (Fig. 1M). Consistent with aberrant activation and translocation, in both A• oligomer-treated primary hippocampal neurons and APPsw Tg2576 mice, pPAK labeled granular structures in cell bodies and neurites in contrast to untreated neurons and nontransgenic mice where diffuse cytosolic PAK was maintained (Fig. 7).

A• is widely believed to be a central causative factor in AD; however, it remains unclear how A• causes synaptic dysfunction, synapse loss, and neuronal degeneration. Our results suggest one mechanism involves aberrant ectopic oligomer-induced activation, translocation, and loss of cytosolic PAKs, which leads to a loss of PAK available for normal coupling to PAK-mediated synapse stabilizing and synaptogenic signaling. In 22-monthold Tg2576 transgene-positive (Tg2576•) and -negative control mice on a high n-6 and low n-3 fatty acid diet that enhances transgene-dependent loss of the actin-binding spine protein, Drebrin and PSD-95 (39), activated pPAKs1–3 were • 70% decreased in cytosol (p • 0.001, Fig. 2). Furthermore, the pPAK ratio of membrane to cytosol in Tg2576• was significantly elevated when compared with Tg2576• controls, suggesting a steady state of persistent aberrant PAK translocation. We previously reported neuritic elevation of aberrant pPAK proximal to plaques (18). A loss of synaptic spine stability in aged Tg2576 on normal mouse chow is accentuated by proximity to plaques and can be observed with multiphoton microscopy in vivo (26). These effects could be oligomer-related as oligomer-specific A11 staining is concentrated in a peri-plaque location (24). Consistent with this, spine loss occurs very early and precedes plaques in APP transgenics (40). Acutely, in vitro, although A• oligomer directly induced PAK activation, there was an aberrant redistribution of pPAK to neurites, membranes, and granular structures (Fig. 3). Because active PAK induces LIMK1 phosphorylation and inactivation of the actin-severing

protein cofilin, one might predict increased F-actin. However, in our experiment, F-actin was rapidly reduced by 7 h, suggesting cofilin was activated, not inactivated. This reduced F-actin was accompanied by altered neuritic morphology, whereas the synaptic marker PSD-95 was also reduced in A• oligomer-treated cultured neurons (Fig. 4).

We sought to clarify where Rac/PAK changes fit in the mechanism of A• oligomer mediated synaptic loss. Rac activation is one of the earliest events following A• oligomer treatment (41). Our data suggest that the rapid activation and translocation of Rac1 and PAK may initiate or contribute to synaptic dysfunction and excitatory synapse loss in AD. Dendritic spine density is closely related to the degree of interneuronal connectivity, whereas the size of spines is correlated with the size of excitatory synapses (42), e.g. synapses that A• oligomer targets (25) associated with reduced LTP and glutamatergic transmission (43). Because PSD-95 clusters NMDA receptors, our results are also likely related to regulation of the surface expression and endocytosis of NMDA-type glutamate receptors and loss of NR2B Tyr(P)-1472 by A• aggregates (44), which have been recently reported to bind NMDA receptors (28). In vitro treatment of primary hippocampal neurons with A• oligomers results in an NMDA receptor-dependent loss of dendritic spines and the dendritic spine marker Drebrin (2,28), reminiscent of Drebrin and NMDA receptor loss in APP transgenic mice (Tg2576) on the diet used in this study (39). Synapse loss and cognitive deficits in APP transgenic mice (33) and oligomer-induced LTP deficits in vitro (32) both require Fyn kinase. We found that the Src/Fyn kinase inhibitor PP2 effectively prevented oligomer-induced Rac/PAK translocation but not loss of the Fyn target pNR2B. This implies that Fyn is independent of or downstream from NMDA receptor events but upstream from PAK pathway defects. Although the Fyn target regulating Rac/PAK signaling is unknown, the upstream Rac activator Tiam1 is known to be tyrosine-phosphorylated and activated by Src family kinases (32) and required for A• -induced Rac activation (45). Tiam1 couples NMDA receptor activation to activity-dependent and Ephrin receptor-dependent dendritic spine formation mediated in part by Rac/PAK signaling. Furthermore, Tiam1 activation of Rac can act both upstream and downstream of phosphatidylinositol 3-kinase (46). Collectively, our data and the literature suggest a scheme in which Fyn lies downstream from NMDA receptors but upstream from Tiam1/Rac1/PAK, a pathway regulating dendritic spine actin (Fig. 8).

Although NMDA receptors are implicated, more than one receptor may contribute to A• oligomer signaling. For example, A• -induced NR2B endocytosis is both NMDA and • $_7$-nicotinic-dependent and correlates with reduced pNR2B Tyr-1472 (44). APP itself binds PAK through APP C-terminal domains requiring Asp-664 and is another candidate receptor that may be involved in age-dependent PAK signaling alterations similar to those we describe. PAK, LTP, and cognitive deficits are correlated in amyloid-accumulating APP Tg mice lacking the C-terminal Asp-664 mutation (47). These results support the hypothesis that aberrant PAK signaling is involved in LTP and cognitive deficits.

Limiting excessive PAK activation with a dominant-negative PAK construct corrected excessive spine numbers, LTP, and cognitive deficits in a fragile X transgenic model (48) suggesting that the excessive PAK activation could be a therapeutic target. Similar to the pattern with active PAK, active LIMK1 is found in dystrophic neurites and clusters of neurons in AD, whereas excessive downstream activation of LIMK1, cofilin inactivation, and dystrophic neurites occurred as a rapid response to A• fibril treatment (49). Compounds targeting PAK activation in AD might have a narrow therapeutic window because PAKs play important roles in cognition and many other cell functions. Furthermore, our data showed that functional WT-PAK but not dominant-negative kinase-dead PAK protected from oligomer-induced spine and PSD-95 loss. Because active WT-PAK inactivates cofilin through active LIMK1, our results are consistent with observations that constitutive expression of inactive cofilin (nonphosphorylated cofilin S3D) can prevent chronic low dose A• oligomer-mediated spine

loss in vitro (2). Collectively, these results suggest that mitigating A• oligomer action in aberrant Rac • PAK signaling may provide therapeutically useful approaches to inhibiting A• oligomer-induced PAK signaling deficits and synaptic dysfunction in AD. Our observations emphasize the complexity of PAK dysregulation in AD and AD models, implicating not only loss of cytosolic PAK but also its aberrant activation and translocation in the loss of dendritic spines contributing to memory loss. Because anti-A• antibody (18) and the anti-oligomer agent dietary curcumin effectively control aberrant PAK translocation in vitro and in vivo, targeting upstream factors, such as oligomers, may be less likely to interfere with cognition than direct targeting of downstream PAK.

Acknowledgments

We thank the patients and families who generously donated brain tissue samples for this research via the Neuropathology Core of the UCLA Alzheimer Disease Research Center (Dr. H. Vinters was supported by National Institutes of Health Grant P50 AG16570) and the University of Southern California Neuropathology Alzheimer Disease Research Center Core (Dr. C. A. Miller was supported by National Institutes of Health Grant P50 AG05142). We thank Dr. M. J. Schibler at UCLA Brain Research Institute for confocal images assistance. We also thank B. Hudspeth, P. P. Chen, and M. Jones for their technical expertise.

REFERENCES

1. Lue L-F, Kuo Y-M, Roher AE, Brachova L, Shen Y, Sue L, Beach T, Kurth JH, Rydel RR, Rogers J. Am. J. Pathol 1999;155:853–862. [PubMed: 10487842]
2. Shankar GM, Bloodgood BL, Townsend M, Walsh DM, Selkoe DJ, Sabatini BL. J. Neurosci 2007;27:2866–2875. [PubMed: 17360908]
3. McLean CA, Cherny RA, Fraser FW, Fuller SJ, Smith MJ, Beyreuther K, Bush AI, Masters CL. Ann. Neurol 1999;46:860–866. [PubMed: 10589538]
4. Walsh DM, Klyubin I, Fadeeva JV, Cullen WK, Anwyl R, Wolfe MS, Rowan MJ, Selkoe DJ. Nature 2002;416:535–539. [PubMed: 11932745]
5. Buttini M, Akeefe H, Lin C, Mahley RW, Pitas RE, Wyss-Coray T, Mucke L. Neuroscience 2000;97:207–210. [PubMed: 10799751]
6. Westerman MA, Cooper-Blacketer D, Mariash A, Kotilinek L, Kawarabayashi T, Younkin LH, Carlson GA, Younkin SG, Ashe KH. J. Neurosci 2002;22:1858–1867. [PubMed: 11880515]
7. Buttini M, Yu GQ, Shockley K, Huang Y, Jones B, Masliah E, Mallory M, Yeo T, Longo FM, Mucke L. J. Neurosci 2002;22:10539–10548. [PubMed: 12486146]
8. Purpura DP. Science 1974;186:1126–1128. [PubMed: 4469701]
9. Blanpied TA, Ehlers MD. Biol. Psychiatry 2004;55:1121–1127. [PubMed: 15184030]
10. Moolman DL, Vitolo OV, Vonsattel JP, Shelanski ML. J. Neurocytol 2004;33:377–387. [PubMed: 15475691]
11. Stachel SJ, Coburn CA, Steele TG, Jones KG, Loutzenhiser EF, Gregro AR, Rajapakse HA, Lai MT, Crouthamel MC, Xu M, Tugusheva K, Lineberger JE, Pietrak BL, Espeseth AS, Shi XP, Chen-Dodson E, Holloway MK, Munshi S, Simon AJ, Kuo L, Vacca JP. J. Med. Chem 2004;47:6447–6450. [PubMed: 15588077]
12. Hayashi K, Ohshima T, Mikoshiba K. Mol. Cell. Neurosci 2002;20:579–594. [PubMed: 12213441]
13. Threadgill R, Bobb K, Ghosh A. Neuron 1997;19:625–634. [PubMed: 9331353]
14. Li Z, Van Aelst L, Cline HT. Nat. Neurosci 2000;3:217–225. [PubMed: 10700252]
15. Ruchhoeft ML, Ohnuma S, McNeill L, Holt CE, Harris WA. J. Neurosci 1999;19:8454–8463. [PubMed: 10493746]
16. Boda B, Alberi S, Nikonenko I, Node-Langlois R, Jourdain P, Moosmayer M, Parisi-Jourdain L, Muller D. J. Neurosci 2004;24:10816–10825. [PubMed: 15574732]
17. Hayashi ML, Choi SY, Rao BS, Jung HY, Lee HK, Zhang D, Chattarji S, Kirkwood A, Tonegawa S. Neuron 2004;42:773–787. [PubMed: 15182717]

18. Zhao L, Ma QL, Calon F, Harris-White ME, Yang F, Lim GP, Morihara T, Ubeda OJ, Ambegaokar S, Hansen JE, Weisbart RH, Teter B, Frautschy SA, Cole GM. Nat. Neurosci 2006;9:234–242. [PubMed: 16415866]
19. Calon F, Lim GP, Yang F, Morihara T, Teter B, Ubeda O, Rostaing P, Triller A, Salem N Jr, Ashe KH, Frautschy SA, Cole GM. Neuron 2004;43:633–645. [PubMed: 15339646]
20. Ma QL, Lim GP, Harris-White ME, Yang F, Ambegaokar SS, Ubeda OJ, Glabe CG, Teter B, Frautschy SA, Cole GM. J. Neurosci. Res 2006;83:374–384. [PubMed: 16385556]
21. Zenke FT, King CC, Bohl BP, Bokoch GM. J. Biol. Chem 1999;274:32565–32573. [PubMed: 10551809]
22. Walsh DM, Townsend M, Podlisny MB, Shankar GM, Fadeeva JV, Agnaf OE, Hartley DM, Selkoe DJ. J. Neurosci 2005;25:2455–2462. [PubMed: 15758153]
23. Lesne S, Koh MT, Kotilinek L, Kayed R, Glabe CG, Yang A, Gallagher M, Ashe KH. Nature 2006;440:352–357. [PubMed: 16541076]
24. Kayed R, Head E, Thompson JL, McIntire TM, Milton SC, Cotman CW, Glabe CG. Science 2003;300:486–489. [PubMed: 12702875]
25. Lacor PN, Buniel MC, Chang L, Fernandez SJ, Gong Y, Viola KL, Lambert MP, Velasco PT, Bigio EH, Finch CE, Krafft GA, Klein WL. J. Neurosci 2004;24:10191–10200. [PubMed: 15537891]
26. Spires TL, Meyer-Luehmann M, Stern EA, McLean PJ, Skoch J, Nguyen PT, Bacskai BJ, Hyman BT. J. Neurosci 2005;25:7278–7287. [PubMed: 16079410]
27. Counts SE, Nadeem M, Lad SP, Wuu J, Mufson EJ. J. Neuropathol. Exp. Neurol 2006;65:592–601. [PubMed: 16783169]
28. Lacor PN, Buniel MC, Furlow PW, Clemente AS, Velasco PT, Wood M, Viola KL, Klein WL. J. Neurosci 2007;27:796–807. [PubMed: 17251419]
29. Parnas D, Haghighi AP, Fetter RD, Kim SW, Goodman CS. Neuron 2001;32:415–424. [PubMed: 11709153]
30. Hing H, Xiao J, Harden N, Lim L, Zipursky SL. Cell 1999;97:853–863. [PubMed: 10399914]
31. Penzes P, Beeser A, Chernoff J, Schiller MR, Eipper BA, Mains RE, Huganir RL. Neuron 2003;37:263–274. [PubMed: 12546821]
32. Lambert MP, Barlow AK, Chromy BA, Edwards C, Freed R, Liosatos M, Morgan TE, Rozovsky I, Trommer B, Viola KL, Wals P, Zhang C, Finch CE, Krafft GA, Klein WL. Proc. Natl. Acad. Sci. U. S. A 1998;95:6448–6453. [PubMed: 9600986]
33. Chin J, Palop JJ, Puolivali J, Massaro C, Bien-Ly N, Gerstein H, Scearce-Levie K, Masliah E, Mucke L. J. Neurosci 2005;25:9694–9703. [PubMed: 16237174]
34. Nakazawa T, Komai S, Tezuka T, Hisatsune C, Umemori H, Semba K, Mishina M, Manabe T, Yamamoto T. J. Biol. Chem 2001;276:693–699. [PubMed: 11024032]
35. Yang F, Lim GP, Begum AN, Ubeda OJ, Simmons MR, Ambegaokar SS, Chen PP, Kayed R, Glabe CG, Frautschy SA, Cole GM. J. Biol. Chem 2005;280:5892–5901. [PubMed: 15590663]
36. Lim GP, Yang F, Chu T, Gahtan E, Ubeda O, Beech W, Overmier JB, Hsiao Ashe K, Frautschy SA, Cole GM. Neurobiol. Aging 2001;22:983–991. [PubMed: 11755007]
37. Nakayama AY, Harms MB, Luo L. J. Neurosci 2000;20:5329–5338. [PubMed: 10884317]
38. Ramakers GJ. Trends Neurosci 2002;25:191–199. [PubMed: 11998687]
39. Calon F, Lim GP, Morihara T, Yang F, Ubeda O, Salem N Jr, Frautschy SA, Cole GM. Eur. J. Neurosci 2005;22:617–626. [PubMed: 16101743]
40. Jacobsen JS, Wu CC, Redwine JM, Comery TA, Arias R, Bowlby M, Martone R, Morrison JH, Pangalos MN, Reinhart PH, Bloom FE. Proc. Natl. Acad. Sci. U. S. A 2006;103:5161–5166. [PubMed: 16549764]
41. Chromy BA, Nowak RJ, Lambert MP, Viola KL, Chang L, Velasco PT, Jones BW, Fernandez SJ, Lacor PN, Horowitz P, Finch CE, Krafft GA, Klein WL. Biochemistry 2003;42:12749–12760. [PubMed: 14596589]
42. Newey SE, Velamoor V, Govek EE, Van Aelst L. J. Neurobiol 2005;64:58–74. [PubMed: 15884002]
43. Kamenetz F, Tomita T, Hsieh H, Seabrook G, Borchelt D, Iwatsubo T, Sisodia S, Malinow R. Neuron 2003;37:925–937. [PubMed: 12670422]

44. Snyder EM, Nong Y, Almeida CG, Paul S, Moran T, Choi EY, Nairn AC, Salter MW, Lombroso PJ, Gouras GK, Greengard P. Nat. Neurosci 2005;8:1051–1058. [PubMed: 16025111]
45. Mendoza-Naranjo A, Gonzalez-Billault C, Maccioni RB. J. Cell Sci 2007;120:279–288. [PubMed: 17200137]
46. Tolias KF, Bikoff JB, Burette A, Paradis S, Harrar D, Tavazoie S, Weinberg RJ, Greenberg ME. Neuron 2005;45:525–538. [PubMed: 15721239]
47. Nguyen TV, Galvan V, Huang W, Banwait S, Tang H, Zhang J, Bredesen DE. J. Neurochem 2008;104:1065–1080. [PubMed: 17986220]
48. Hayashi ML, Rao BS, Seo JS, Choi HS, Dolan BM, Choi SY, Chattarji S, Tonegawa S. Proc. Natl. Acad. Sci. U. S. A 2007;104:11489–11494. [PubMed: 17592139]
49. Heredia L, Helguera P, de Olmos S, Kedikian G, Sola Vigo F, LaFerla F, Staufenbiel M, de Olmos J, Busciglio J, Caceres A, Lorenzo A. J. Neurosci 2006;26:6533–6542. [PubMed: 16775141]
50. Nikolic M, Chou MM, Lu W, Mayer BJ, Tsai LH. Nature 1998;395:194–198. [PubMed: 9744280]
51. Frasca G, Carbonaro V, Merlo S, Copani A, Sortino MA. J. Neurosci. Res 2008;86:350–355. [PubMed: 17828768]
52. Liang X, Draghi NA, Resh MD. J. Neurosci 2004;24:7140–7149. [PubMed: 15306647]
53. Kihara T, Shimohama S, Sawada H, Honda K, Nakamizo T, Shibasaki H, Kume T, Akaike A. J. Biol. Chem 2001;276:13541–13546. [PubMed: 11278378]

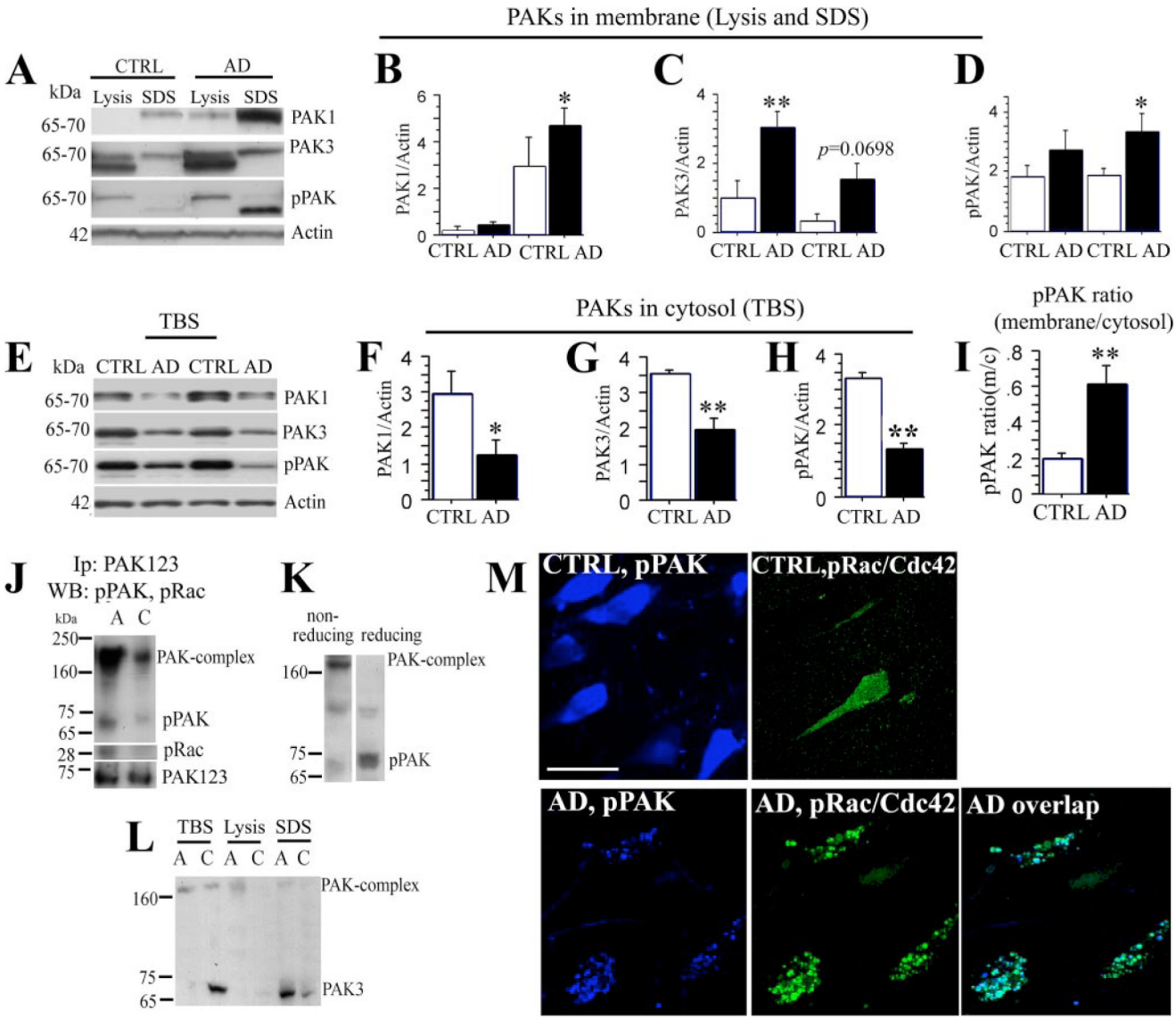

FIGURE 1. PAK/Rac/Cdc42 translocation in Alzheimer disease

A–H, AD brain tissues from temporal cortex sections were fractionated. The TBS and insoluble-membrano-cytoskeletal (lysis and SDS) fractions separated by SDS-polyacrylamide gel were Western-blotted with anti-PAK1, PAK3, phospho-PAK1–3 (Ser-423) (pPAK) and • -actin antibodies. Lysis and SDS fractions (A) and TBS fractions (E) for PAK1, PAK3, pPAK, and • -actin are shown. CTRL, control. Quantification of immunoblots showed significant changes in • -actin normalized PAK1 (B, *, p • 0.05), PAK3 (C, **, p • 0.01), pPAK in insoluble fractions (D, *, p • 0.05) and in TBS-soluble fractions (F, PAK1, *, p • 0.05; G, PAK3, **, p • 0.01; H, pPAK, **, p • 0.01), and the ratio of pPAK-insoluble versus soluble fractions (I, **, p • 0.01). • -Actin was used for normalization for protein loading. J, immunoprecipitation (IP) analysis of PAK and pRac1/Cdc42 co-translocation in hippocampus in AD. A, AD; C, control. Pooled membrane pellet fractions extracted with lysis buffer from AD or normal human hippocampi were immunoprecipitated with an anti-PAK123 antibody, followed by Western blot detection of pPAK and pRac1/Cdc42. Both levels of pPAK and pRac1/Cdc42 monomer were increased in AD patients as compared with controls. For another strong pPAK immunoreactive band between 160- and 250-kDa size, a potential PAK complex was observed

on the same blot and was also increased in AD samples. K, higher molecular weight immunoreactive pPAK present on our standard weakly reducing gels (left) and replaced by lower molecular weight predicted pPAK monomer after boiling with DTT. L, PAK3 translocation in AD brain. PAK3 were elevated in SDS membrane extracts from pooled individual AD cases (n • 5) when compared with normal controls (n • 5), whereas PAK3 in TBS fractions (cytosol) was decreased in the same AD samples. A, AD; C, control. M, active PAK and pRac/Cdc42 were co-translocated in the hippocampus of patients with AD. Anti-pPAK labeled diffuse cytosolic pPAK in normal controls but focal granular structures in AD brain. Anti-pRac labeled weakly in normal controls and when detected labeling was diffuse. Biotinylated pPAK (blue) and phospho-Rac/Cdc42 (green) co-translocation was detected by confocal microscopy in hippocampus from AD brain. Abnormal granular pPAK structures were nearly completely co-localized with pRac/Cdc42 at the membrane of neurons; scale bar, 25 • m.

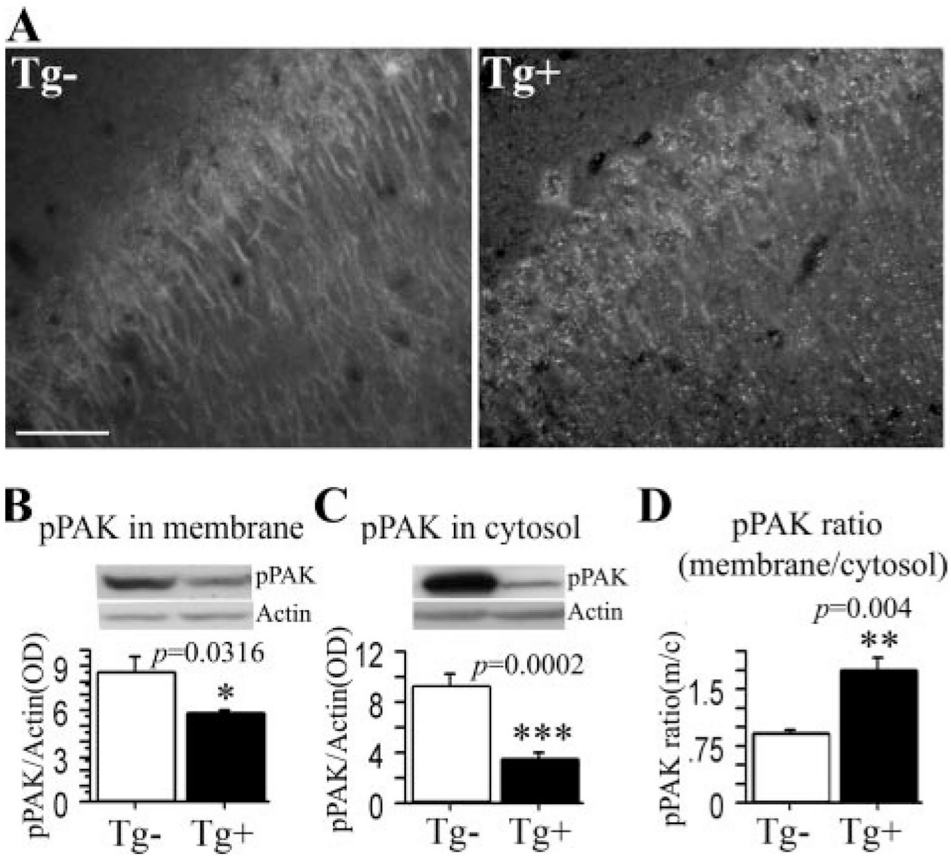

FIGURE 2. PAK translocation in Tg2576 mice

A, immunofluorescent staining of PAK translocation in hippocampus of Tg2576 mice. 22-Month-old Tg2576 transgenic Tg• and control Tg• mice were stained with anti-pPAK antibody. Anti-pPAK identified a loss of diffuse perikaryal and dendritic labeling along with granular structures in Tg2576 transgenic Tg• mice; scale bar, 25 • m. B–D, Western immunoblot analysis of PAK translocation in the cortex in aged Tg2576 mice. The levels of pPAK were significantly reduced in membrane and cytosol from Tg2576 Tg• mice when compared with control Tg2576 Tg• mice (B, *, p • 0.05; C, ***; p • 0.001), and in contrast, the pPAK ratio of membrane to cytosol was significantly increased in Tg2576 Tg• mice when compared with control Tg2576 Tg• mice (D, ***, p • 0.001).

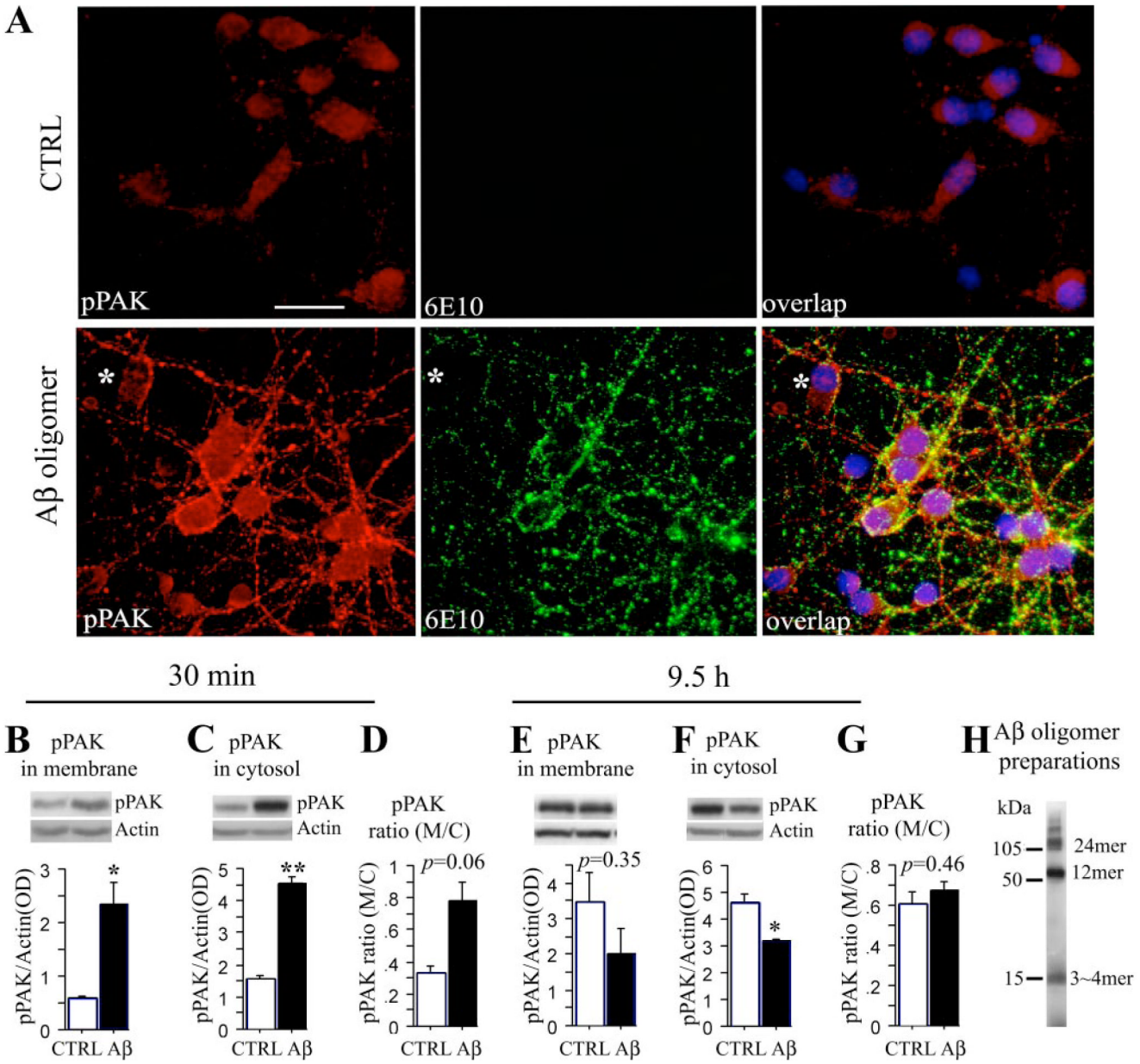

FIGURE 3. A• $_{42}$ oligomer-induced PAK activation and translocation in primary neurons

A, immunofluorescent staining of PAK activation and translocation induced by A• $_{42}$ oligomer in primary hippocampal neurons. Primary hippocampal neurons 7 DIV were treated with 100 nM A• oligomers for 30 min and then stained with anti-pPAK (red), anti-A• (6E10, green), and the purple nuclear stain, 4•,6-diamidino-2-phenylindole; scale bar, 25 • m. CTRL, control. B–G, Western immunoblot analysis of PAK activation and translocation induced by A• $_{42}$ oligomer in primary hippocampal neurons. Hippocampal neurons 7 DIV were treated with 250 nM of A• oligomers and Western-blotted with anti-pPAK antibody. pPAK levels were significantly increased in membrane and cytosol (M/C) fractions after 30 min in A• $_{42}$ oligomer-treated neurons when compared with controls (B, *, p • 0.05; C, **, p • 0.01). The pPAK ratio of membrane to cytosol had a strong trend to increase by 30 min in A• $_{42}$ oligomer-treated neurons when compared with controls (D, p • 0.0630). In contrast pPAK levels were no longer increased in membrane fractions (E) and were significantly reduced in cytosol fraction by 9.5

h (F, *, p • 0.05). As a result, the membrane/cytosol ratio was no longer significantly altered (G). H, A• oligomer preparations detected by 6E10 antibody.

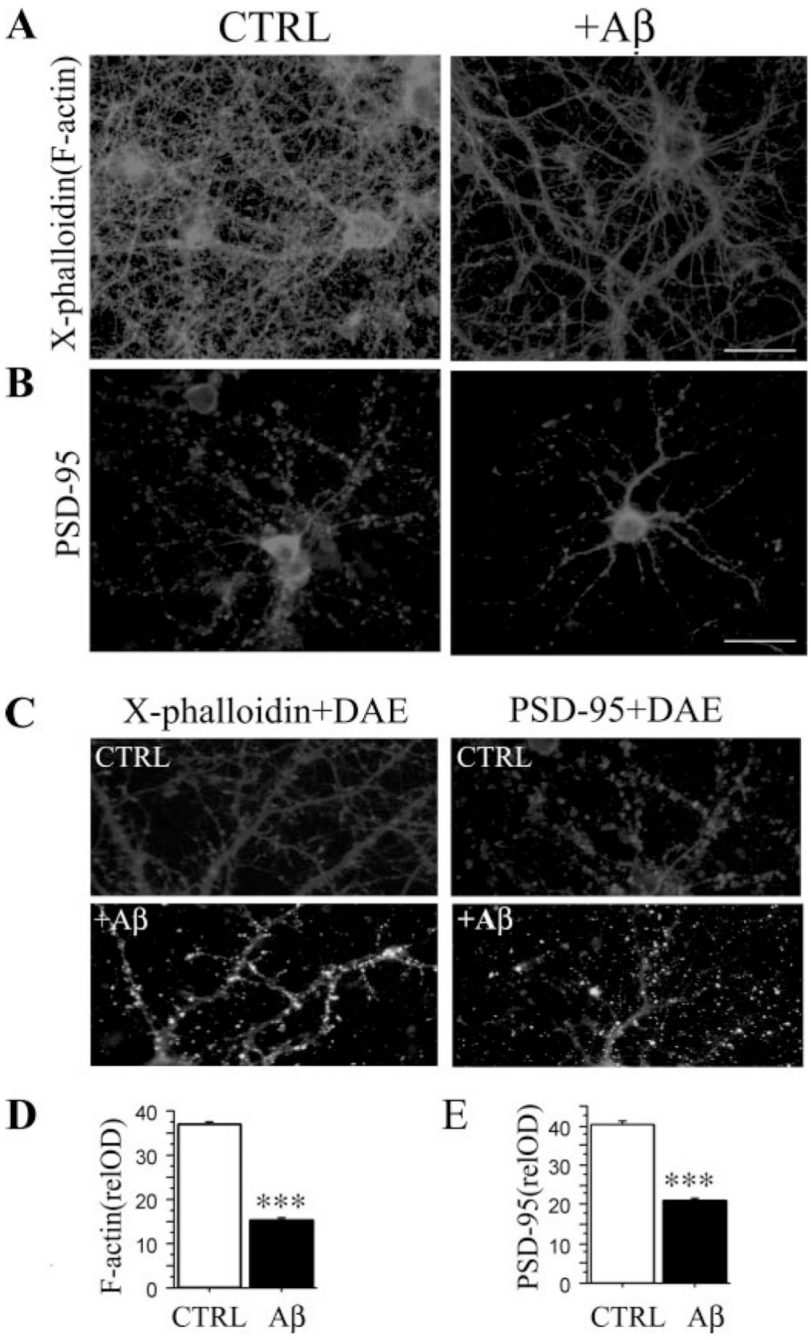

FIGURE 4. Reduction of dendrites and dendritic spines in A• $_{42}$ oligomer-treated primary neurons

A, A• $_{42}$ oligomers (7 h) induced decreases in Texas-red-X-phalloidin labeled F-actin in dendrites and dendritic spines of A• oligomer-treated mature 19 DIV hippocampal neurons. The density of dendritic spines from image analysis of F-actin along dendrites confirmed significantly reduced F-actin labeling of spines in A• $_{42}$ oligomer-treated neurons when compared with controls (D, ***, p • 0.001); scale bar, 25 • m. B and E, A• $_{42}$ oligomers induced decreases in PSD-95 in A• oligomer-treated mature hippocampal neurons. Primary hippocampal neurons were stained with anti-PSD-95 (gray) and anti-A• (white) antibodies. Quantification of PSD-95 along dendrites revealed a significant loss (E, ***,p • 0.001);

scalebar,25 • m. C, enlargement of dendrites and dendritic spines stained by X-phalloidin (gray), PSD-95 (gray), and an anti-A• polyclonal antibody, DAE (white). CTRL, control.

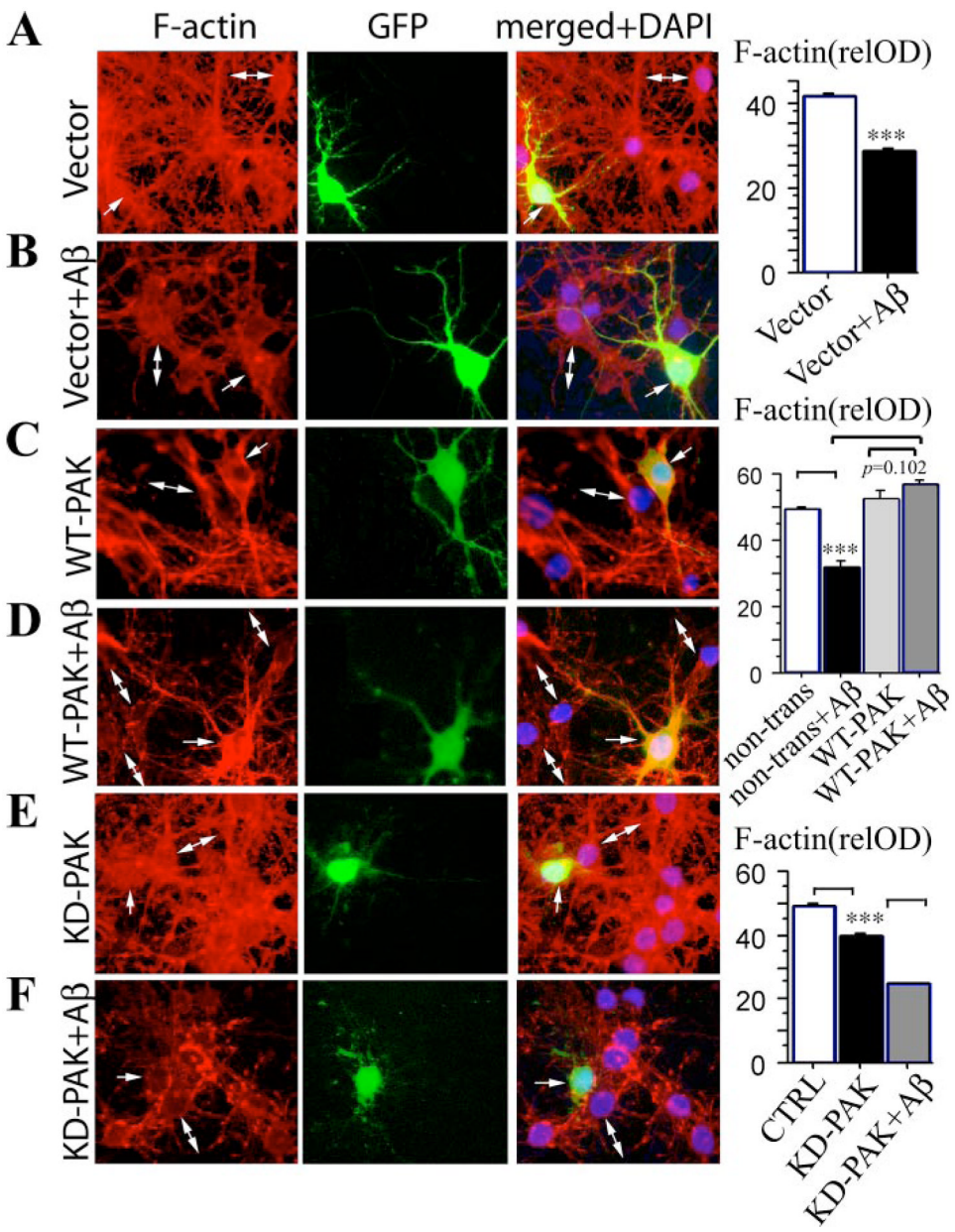

FIGURE 5. WT-PAK1, but not kinase-dead PAK1 limited A• $_{42}$ oligomer-induced reduction of dendrites in primary

Hippocampal neurons 7 DIV were transfected with control pcDNA3-EGFP-vector alone (Vector Laboratories) (A and B), wild type (WT), pcDNA3-EGFP-Pak1-WT (WT-PAK, C and D), or kinase-dead pcDNA3-EGFP-PAK1-K299A (KD-PAK, E and F), treated by 100 n$_M$ A• $_{42}$ oligomer for 7 h (B, D and F) and stained for F-actin (red). Nuclei were 4•,6-diamidino-2-phenylindole-stained (DAPI, blue). Transfected cells express green GFP (middle column), which was shown merged with F-actin images. In non-A• $_{42}$-treated neurons, F-actin staining is robust (A, C, and E) but markedly reduced after A• $_{42}$ oligomer treatment (B, D, and F). Transfected WT-PAK cells were protected from A• $_{42}$ oligomer-induced F-actin loss compared with adjacent nontransfected cells (D). In contrast, the GFP vector transfected cells and the KD-PAK transfected cells did not show any protection against A• $_{42}$ oligomer-induced F-actin loss compared with adjacent nontransfected cells (B and F). F-actin quantification

panels are on the right. Single arrow indicates transfected cells; double arrows indicate nontransfected cells; scale bar, 25 • m. CTRL, control.

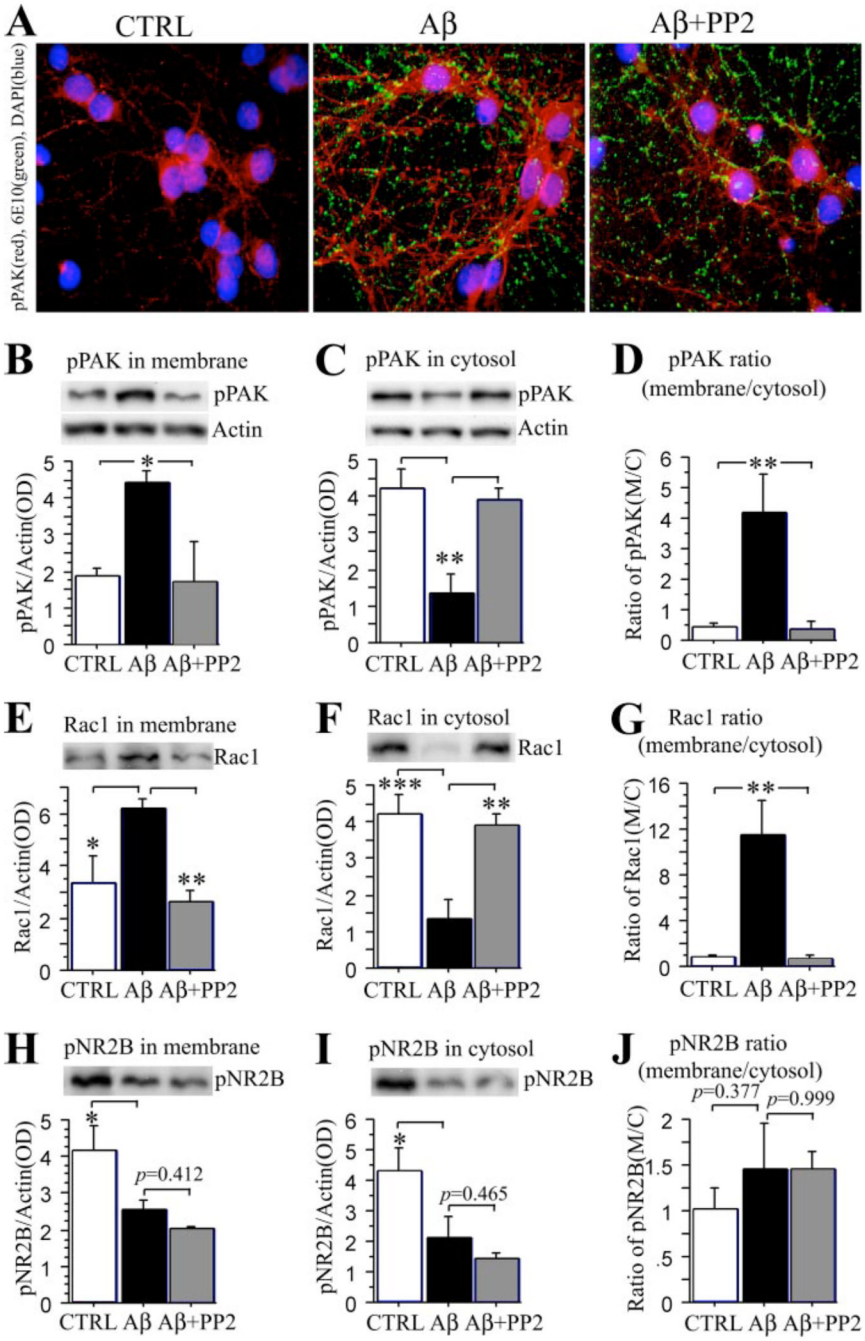

FIGURE 6. Src family tyrosine kinase inhibitor PP2 significantly blocked A• $_{42}$-induced PAK/Rac translocation but not NR2B loss in primary neurons

Hippocampal neurons 10 DIV were treated with 100 n$_{M}$ A• $_{42}$ oligomers or A• $_{42}$ oligomers plus 10 • $_{M}$ PP2 for 5 h, and pPAK was evaluated by immunofluorescent staining and Western blot. A, immunofluorescent pPAK staining revealed PP2 blocked activation and translocation induced by A• $_{42}$ oligomers in primary hippocampal neurons. B–D, PP2 prevents A• $_{42}$ oligomer-induced pPAK translocation. pPAK protein levels, measured by Western blot, were significantly increased in membrane and decreased in cytosol fractions by oligomers, whereas PP2 significantly blocked this pPAK translocation when compared with controls (B, *, p • 0.05; C, **, p • 0.01). The ratio of pPAK in the membrane relative to in the cytosol was

significantly increased in A• $_{42}$ oligomer-treated neurons but not in the presence of PP2 (D, **, p • 0.01). E–G, PP2 prevents A• $_{2}$ oligomer-induced Rac1 translocation. Rac1 protein levels, measured by Western blot, were significantly increased in membrane (E, *, p • 0.05) and decreased in cytosol fractions by oligomer treatment (F, ***, p • 0.001), whereas PP2 blocked this Rac1 translocation (E and F, **, p • 0.01) as well as the increased Rac1 membrane/cytosol ratio (G, **, p • 0.01). H–J, Western immunoblot analysis of pNR2B. pNR2B levels were significantly decreased in both membrane and cytosol fractions (H and I, *, p • 0.05); PP2 had no effect on this loss or (p • 0.05) the pNR2B membrane to cytosol ratio (J, p • 0.05). CTRL, control.

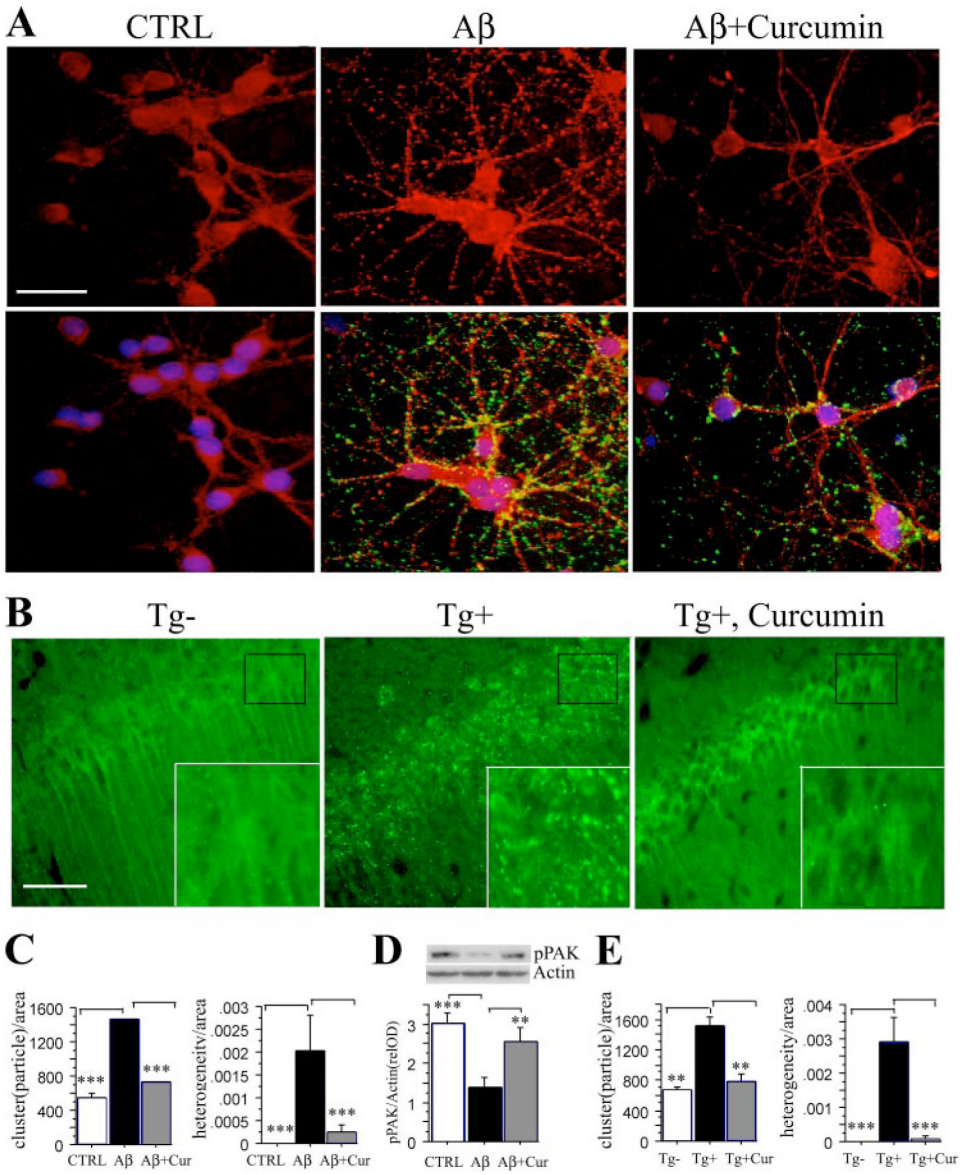

FIGURE 7. Curcumin suppressed pPAK translocation

A, C, and D, curcumin suppressed pPAK translocation in primary neurons. Hippocampal neurons 7 DIV were treated with 100 nM A• 42 oligomers or A• 42 oligomers plus 0.5 • M curcumin. After 30 min of treatment (or 2 h; data not shown), the active PAK (red) assessed by immunostaining appeared translocated from cytosol in untreated controls (CTRL) to membrane and neurites with A•, but this translocation was suppressed by curcumin. Image analysis of the granular clustering and heterogeneity of this pPAK staining were used as quantitative measures of this effect (C); scale bar, 25 • m. Curcumin also reduced punctate anti-A• antibody staining (green, lower panels, A), which decorated neuronal cell bodies and processes. Western analysis showed oligomer-induced deficits in cytosolic active PAK with chronic treatment (9.5–48 h), which was significantly blocked by curcumin (D). B and E, curcumin suppressed pPAK translocation evaluated by ICC in aged Tg2576 mice. 22-Month-old Tg2576 transgenic Tg•, Tg• fed with curcumin, and Tg• mice (n • 4) were stained with anti-pPAK antibody. Anti-pPAK immunofluorescence staining labeled diffuse pPAK in Tg• mice with translocation with granular structures in hippocampus in Tg2576 Tg• mice which was

significantly blocked by 500 ppm curcumin in chow from 17 to 22 months. Scale bar, 25 • m. Insets depict PAK translocation with granular structures in Tg2576 Tg• mice compared with Tg• fed with curcumin or Tg• mice. E, image analysis of pPAK clustering and heterogeneity confirm an APP Tg• -induced rise in pPAK translocation that is suppressed by dietary curcumin.

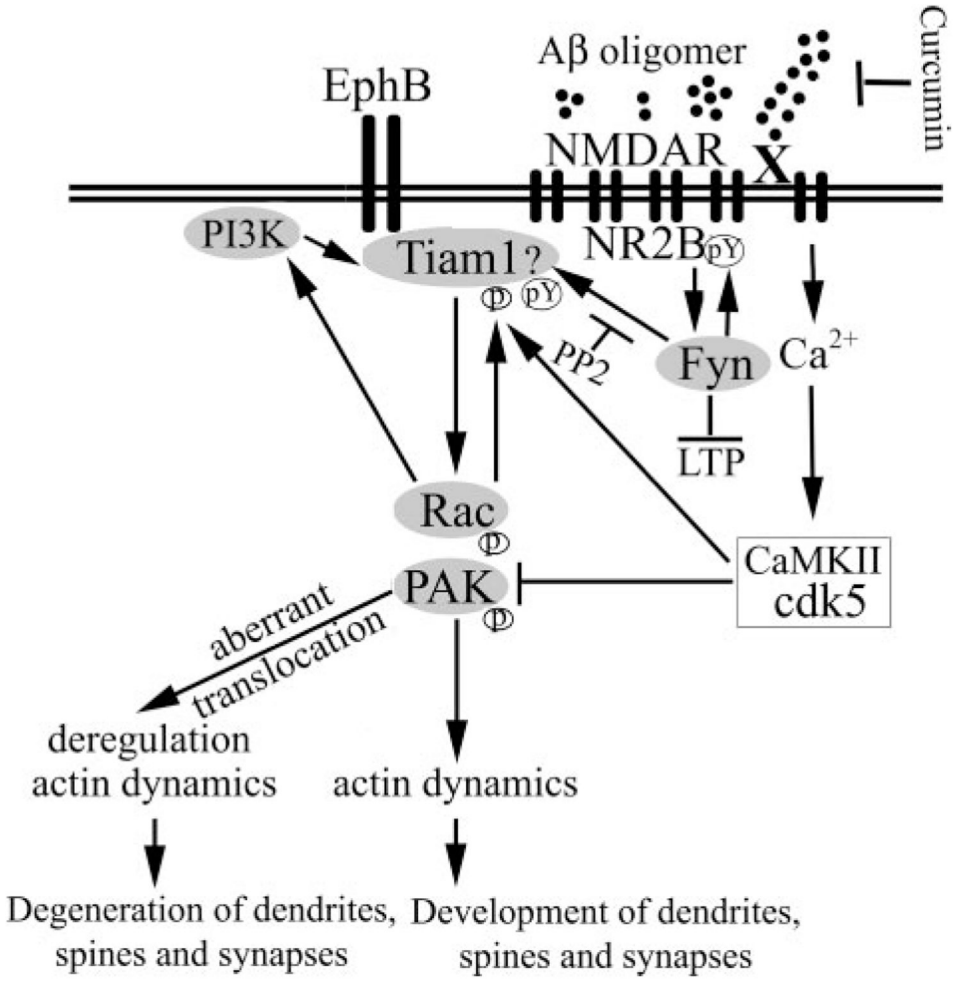

FIGURE 8. Schematic mechanism of A• oligomer-mediated aberrant PAK activation and translocation in Alzheimer disease pathogenesis

Both Ephrin B and NMDA receptors are rapidly down-regulated by A• oligomers (28) and also activate a Tiam1• Rac • PAK pathway that regulates dendritic spine stability and formation through control of actin dynamics, including suppression of the actin-severing protein cofilin reported to mediate oligomer-induced spine loss (1,2). Tiam1 activation is also required for acute A• aggregate-induced Rac activation and translocation (45) that we show accompanies PAK translocation. Tiam1 activation can be achieved by phosphorylation from elevated calcium acting through CaMKII, but PAK is eventually inhibited by calcium-induced calpain activation of Cdk5 (50). PAK could also be activated through direct interaction with candidate A• receptors (X), for example, the amyloid precursor protein (47) or indirectly via Src/Fyn activation of Tiam1. Although the A• receptors are not clearly established, A• -mediated in vivo synaptotoxicity and in vitro LTP deficits are both Fyn kinase- (32,33) and NMDA receptor-dependent (1,2). The Src family kinase Fyn is also physically associated with at least two candidate A• receptors (X), notably integrin receptors (51,52) and • $_7$-nicotinic receptors (53), suggesting they could activate Fyn to mediate deranged downstream Rac/PAK translocation and signaling caused by A• oligomers, which we find blocked by the anti-oligomer drug curcumin. This hypothetical scheme is supported by our data showing that the Src/Fyn inhibitor PP2 blocks the Rac/PAK translocation and loss of dendritic spine F-actin.